Journal of Marine Research, 76, 119–137, 2018

Antarctic Mode Water

by K. Speer[1,2], J.-B. Sallee[3] and V. Pellichero[3]

ABSTRACT

An estimate of Southern Ocean volume in temperature-salinity (T-S) classes is made with a focus on cold water masses south of the Polar Front, at depths shallower than 2,000 m. The volumetric diagram for waters below 5 °C shows a deficit at temperatures near 0 °C and 34.2 psu, surrounded by a ring of larger volumes, related to water mass formation near the Polar Front and near the continental margins as well as mixing effects. The cold, fresh extreme of the Antarctic Intermediate Water T-S relation shows a volumetric maximum, apparently distinct from the interior T-S relationship. We identify this mode as Antarctic Mode Water with a volumetric maximum centered near 2.0 °C and 33.9 psu. This maximum lies on a large-scale ridge of high volume representing the Antarctic Surface Water mixed layers south of the Polar Front, at the northern edge of the seasonal sea-ice cover. Additional maxima on the diagram near freezing temperatures seem to be related to processes operating on the slope and shelf, though the data coverage in these regions is much reduced. The origin of the Antarctic Mode Water is ultimately due to sea-ice melt, which systematically shifts the T-S relation of surface water to lower salinities, whereas its thickness and distribution is linked to circumpolar northward Ekman transport and the eddy fluxes of the Polar Front.

Keywords: Mode Water, Antarctic zone, Polar Front, mixed layer, Winter Water

1. Introduction

The surface mixed layer of the Southern Ocean is broadly driven by the seasonal cycle of heating and cooling due to air–sea interaction. Dong et al. (2007) attributed the large-scale mixed-layer heat budget dominantly to air–sea fluxes, whereas Dong et al. (2009) found that entrainment and Ekman advection was most important for the salinity budget (see also Gordon 1971; Gordon and Huber 1984; Park et al. 1998; Aoki et al. 2006). Ren et al. (2011) revisited the Southern Ocean mixed-layer salinity budget, finding a stronger role for air fluxes, as well as a significant role for sea-ice melt, which cannot be neglected south of the Polar Front. Pellichero et al. (2017) have exploited substantially enhanced sampling in the Antarctic zone and conclude that the sea surface freshwater and heat budgets are dominated

1. Department of Earth, Ocean, and Atmospheric Sciences, and the Geophysical Fluid Dynamics Institute, Florida State University, Tallahassee, Florida, USA.
2. Corresponding author ***e-mail: kspeer@fsu.edu***
3. Laboratoire d'Océanographie et du Climat: Expérimentations et Approches Numériques, Paris, France.

by sea-ice freshwater flux and by the air–sea heat flux. Ekman advection, vertical diffusivity, and vertical entrainment are of secondary importance.

Outside the Antarctic Zone, Sallée et al. (2006; 2008a) emphasized the local importance of the Ekman advection and eddy mixing contributions to surface mixed layers, especially to the development and evolution of Subantarctic Mode Water (SAMW) in the Indian Ocean. These mode waters are found north of the Subantarctic Front (SAF) at a variety of temperatures, salinities, and densities (Hanawa and Talley 2001), and their rate of formation and spread has been estimated using both observations (Sallée et al. 2010a) and models (Cerovečki et al. 2013). In an analysis of mixed-layer depth from Argo profiles across the Southern Ocean, Dong et al. (2008) suggested that spatial variations in SAMW are a result of the spatially variable underlying stratification. Time variations, on the other hand, of SAMW south of Australia were identified by Rintoul and England (2002) to be due to Ekman transport, and Sallée et al. (2010b) linked large-scale inter-annual variations in Southern Ocean surface layer properties to air–sea heat fluxes and Ekman heat transport anomalies related to the Southern Annular Mode.

In the region south of the Polar Front, winter cooling produces virtually complete coverage by sea-ice at its maximum extent, and the sea-ice is a fundamental part of the seasonal thermodynamic balance (Toole 1981; Ren et al. 2011; Pellichero et al. 2017). During summer, sea-ice melts, breaks up, and retreats back to the continent in places. This freshwater input can influence mixed-layer depth and properties in the seasonal ice-covered region (Park et al. 1998; Aoki et al. 2006; Behrendt et al. 2011).

Seasonally deepening mixed layers are well known to occur south of the Polar Front (Gordon and Huber 1990), though their depth is typically rather modest compared with that of SAMW, with maximum values of up to about 300 m near the Polar Front; Toole (1981) provided a very thorough analysis of the distribution and properties of this surface layer and its relation to the seasonally evolving sea-ice field. Strong meridional variations in the separate terms contributing to the upper ocean heat balance were discussed by Faure et al. (2011) for the region south of Africa, and by Aoki et al. (2006) along 140 °E, implicating various balances of local air–sea fluxes, entrainment, lateral mixing, and Ekman advection. Park et al. (1998) investigated surface waters across the Indian Ocean sector and determined that the advection of meltwater from the Weddell Sea was the primary cause for summer freshening.

The surface mixed layers south of the Polar Front show a relatively broad range of temperature from near freezing up to 5 °C or so near the Polar Front (Carmack 1977). Their range of salinity, from roughly 33–34.5 psu, is larger, compared with temperature, in terms of its effect on density. The low salinity and temperature of the mixed layer permits the development of the temperature minimum layer at the base of the wintertime mixed layer, known as Winter Water from the earliest days of Southern Ocean hydrography.

The depth of the temperature minimum (Tmin) shows a more or less steady increase out to the Polar Front (PF), following the gradual progression of sea-ice formation outward from the continent (Fig. 1). Aoki et al. (2006) show that the instantaneous mixed-layer depth and depth of the Tmin are not always the same but evolve according to the local sources of

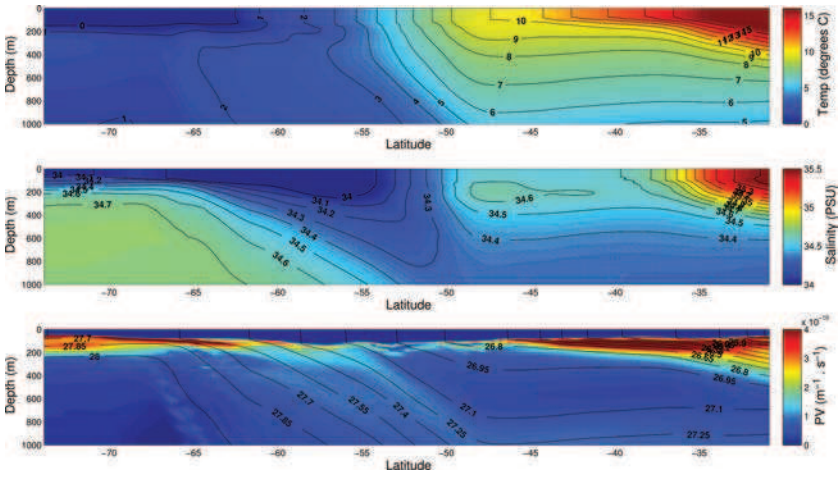

Figure 1. Winter hydrographic section. Monthly MIMOC data averaged over June–Jul–Aug on a line near 160 °W, between 30 °S and 75 °S (Upper, temperature; Middle: salinity; Lower: potential vorticity). Potential vorticity is calculated in the large-scale approximation as f dρ/dz, with neutral density (g/cm^3) overlaid. The extent of the mixed layer is marked by uniformly low PV near the surface, with a deeper layer near 58 °S. The frontal region from 50–60 °S is a smoothed representation of the two main fronts: The Polar Front located at 58 °S and the SAF at about 52 °S.

heat and salt. Winter convection includes a haline component due to freezing seawater and this is thought to contribute to a haline stratification at the base of the mixed layer (Gordon et al. 1984). Near the Polar Front less sea-ice is actually formed (though it often is found there due to lateral drift) and winter mixed-layer deepening may instead be retarded by the previous summer's meltwater.

The meridional salinity gradient in the Tmin layer is notably the opposite that of the surface, with fresher water in the north (Fig. 1; near 200 m depth). In the northern reaches closer to the Polar Front, the underlying warm, salty Circumpolar Deep Water (CDW) is less close to the surface, but also brine rejection effects are attenuated to the north because sea-ice advects with Ekman drift, melts, and cools the surface until ice formation begins, and only then is salinity increased. Toole (1981) pointed out this feedback effect, enhancing the northward penetration of the sea-ice edge in his model.

Whitworth et al. (1998) provide a careful description of water masses in the Antarctic polar ocean region, especially near the slope and shelf, and ascribe variations in the depth of the Winter Water or Tmin to variations in the depth of the CDW underneath, due in turn to wind-driven gyre effects. Deepening of the Tmin layer occurs to the north where the CDW is itself deeper (Fig. 1). On the other hand, approaching the continental margin, surface mixed layers over the slope and shelf can also be quite deep, even deeper than those near the Polar Front. Whitworth et al. (1998) discuss measurements by Fahrbach et al. (1994) and others showing mixed-layer depths or surface water layer thicknesses ranging to depths greater than 500 m.

However, these deep shelf and slope mixed layers are not ubiquitous. Aoki et al. (2006) find, for example, more modest increases in mixed-layer depth near the slope and shelf at 140 °E. Sea-ice processes, melt and brine rejection, dominate the mixed layer forcing over shelf in all Antarctic regions according to the mixed-layer modeling results of Petty et al. (2014), with a smaller air–sea heat flux term and negligible wind effect on mixed-layer evolution. Their model generates mixed layers deeper than 500 m in the Weddell and Ross Seas and in Prydz Bay, in front of the ice shelves, where sea-ice forcing is strongest, and shallower mixed-layer depths elsewhere.

The development of the seasonal mixed layer between the continent and the fronts of the Antarctic Circumpolar Current (ACC) produces a range of depths as well. Deeper mixed layers near the Polar Front are evident in winter data from a hydrographic section near 160 °W generated from the database used here (Fig. 1). Deep mixed layers formed from winter convection are traditional markers of mode waters, extensive areas of similar water type, defined by peaks on a volumetric temperature-salinity (T-S) diagram (Worthington 1981). Mode waters are by definition localized in T-S classes, according to a relation on a T-S diagram or a single water type at a more or less well-defined temperature and salinity. This forms, on a volumetric T-S diagram, a "ridge" in the case of a T-S relation (such as SAMW) or, if the mode water is a particular water type (such as 18 ° Water), it will form a volumetric "peak" (Speer and Forget 2013).

Do the deeper mixed layers south of the Polar Front constitute a mode water? The winter mixed layer along 160 °W (Fig. 1) reaches a maximum depth near 200 m, which is not particularly deep, and the broad range of temperature and salinity consistent with seasonal mixed-layer evolution suggest that volume in T-S classes ought to be spread widely, not confined to a narrow band. That is, deeper surface mixed layers alone do not necessarily make a mode water because properties can vary in a way that spreads the volumetric contributions over a wide range of temperature and salinity, and indeed this seems to be the case for the Antarctic Surface Water. However, the presence of strong lateral mixing and subduction of winter waters produces a reservoir of these waters near the Polar Front, and the contributions of the neighboring surface winter layer together with waters (of similar type) below the mixed-layer base add up to a volumetric mode that we discuss in the following section. This mode also constitutes source water for Antarctic Intermediate Water (AAIW). The spatial distribution of the particular T-S characteristics of the mode illustrates its circumpolar extent.

2. Southern Ocean volumetric diagram

We use the Monthly Isopycnal/Mixed-layer Ocean Climatology (MIMOC) of Schmidtko et al. (2013) to produce an upper ocean southern hemisphere estimate of volume at each water type in bins of 0.05 °C, 0.05 psu, from depths shallower than 2,000 m (Fig. 2). The depth cutoff reflects the maximum depth of the typical Argo profile, but we are in any case focused here on the layers at less than 500 m depth for the most part. The diagram is quite

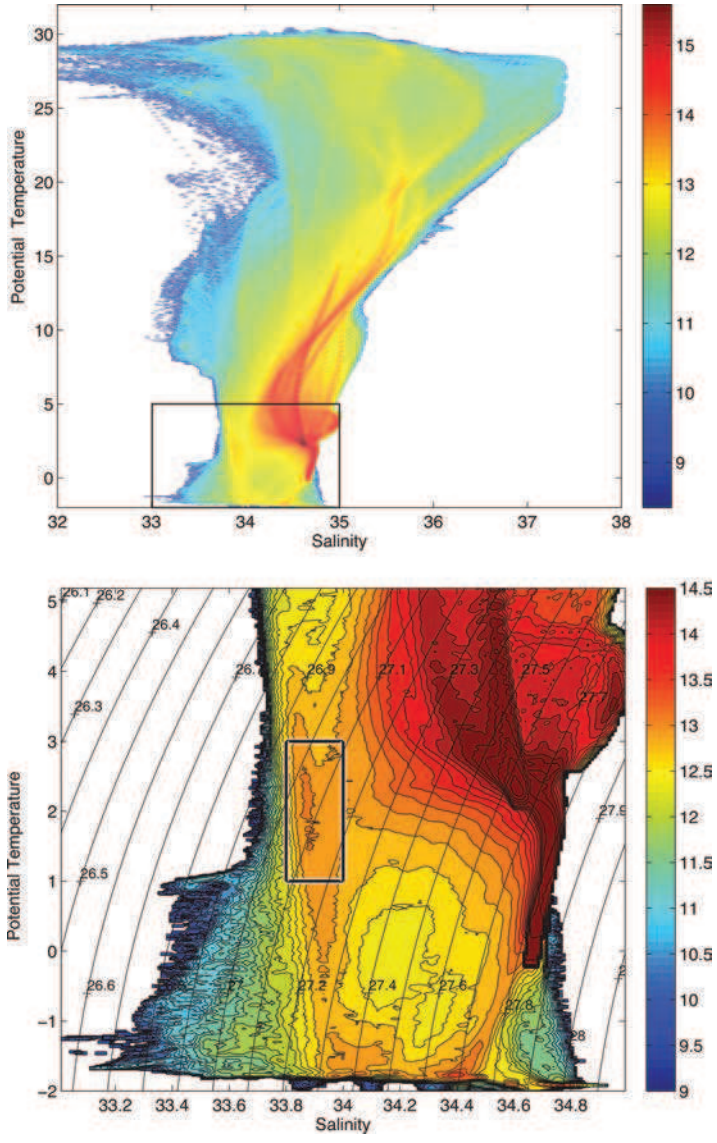

Figure 2. Southern Hemisphere upper ocean (≤2,000 m) T-S volumetric water mass census (upper panel, in m^3; plotted as $\log_{10}$ in each 0.05 °C, 0.05 psu bin) computed from the MIMOC atlas (Schmidtko et al. 2013). The lower panel is a close-up of the area within the black rectangle, or values colder than 5 °C. The rectangle in the lower panel near 2 °C and 33.9 psu indicates the core T-S characteristics of AAMW (i.e., $33.8 \leq S \leq 34$ psu; $1 \leq T \leq 3$ °C). Potential density contours (labeled solid curves) are displayed on the lower panel.

different from a global census (e.g., Worthington, 1981) due both to the depth and latitude (south of the equator) limits. The presence of a depth cutoff removes deep and bottom water contributions away from the Antarctic margins while the latitude cutoff at the equator also eliminates the cold, dense contributions from polar water masses at the high northern latitudes.

The full Southern Hemisphere volumetric diagram encompasses polar to equatorial regions (Fig. 2, upper). Made of multiple minor ridges or branches, it nevertheless sits entirely within Worthington's (1981) central warmer water ridge, at temperatures between about 10 °C and 20 °C. Worthington (1981) called it "cosmopolitan" as it contains water masses from all three major ocean basins. Tropical water masses from various Southern Hemisphere sources appear at temperatures greater than 20 °C (Speer and Forget 2013).

The cold-water diagram (Fig. 2, lower) shows a dominant volumetric peak at 2.2 °C, 34.6 psu, from which a central branch extends to higher temperature: this is the Upper Circumpolar Deep Water (UCDW). On either side are branches extending to warmer water. A weak fresher branch represents the portion of UCDW at the base of AAIW, mainly in the Pacific sector. The high salinity branch arises from the influence of NADW in the South Atlantic sector; however, this branch is suppressed by the 2,000-m depth cutoff, and an isolated maximum artificially appears near 3 °C and 34.9 psu. Below 2 °C, the denser CDW branch extends down toward Antarctic Bottom Water (AABW). CDW and Shelf Water are thought to mix across the Antarctic Slope Front (see review in Whitworth et al. 1998) and a ridge of higher volume appears from near 0 °C and 34.6 psu to freezing and 34.4 psu suggestive of such mixing. This branch is consistent with Modified CDW.

Near the freezing temperature and 34.4 psu, a relatively large volumetric peak appears on the diagram (Fig. 2, lower). As noted earlier, deep surface mixed layers are found close to the continent. Whitworth et al. (1998) mention Fahrbach et al.'s (1994) observation of a 600-m deep ASW layer on the shelf in the southern Weddell Sea, and discuss this observation along with those of several other sections crossing the margin, showing thick layers near the freezing point and 34.4 psu. Such a variation in layer thickness implies a control by dynamics as well as convective processes, because the horizontal density gradient supports geostrophic flow in the Antarctic Slope Front. The presence of a volumetric maximum lends support to the conclusions of Whitworth et al. (1998) that water in the Slope Front mixes along its route, elevating salinity to the point where it becomes easier to mix with denser shelf water, suggesting that water ought to accumulate at this salinity. Beyond this point, denser water tends to spread away from the shelf area as bottom water. We must be cautious, however, about the interpretation of volumetric structure resulting from observations near the margin because the sampling is very uneven (Appendix A).

The primary focus here is the ridge of Antarctic Surface Water (also Modified Antarctic Surface Water) and an associated maximum near 2.0 ° ± 1.0 °C, 33.9 ± 0.1 ppt (Fig. 2, indicated by box in lower panel). This maximum seems rather weak in log coordinates but is about a factor of three larger than the surrounding values. It depends to some extent on the data sampling and averaging; alternatively, the NOAA World Ocean Atlas (Boyer et al.

2013) can be used to produce the volumetric T-S diagram and the result is very similar, with a ridge and maximum also evident. We identify this maximum as Antarctic Mode Water (AAMW). The ridge of higher volume lies on the low salinity side of the diagram and spans a range of temperatures from the freezing point to greater than 3 °C. We define the characteristic T-S range of AAMW based on the volumetric diagram as follows: 1 °C $<$ T $<$ 3 °C and 33.8 psu $<$ S $<$ 34 psu. This is the definition we use for AAMW in subsequent discussion.

The AAMW is at the relatively warm, fresh extreme of mixed-layer depths south of the Polar Front. Both precipitation and sea-ice melt seem to play an important role in the local seasonal salinity budget of the surface mixed layer (Ren et al. 2011; Pellichero et al. 2017; 2018). Ultimately, however, the salinity gradients at the base of the mixed layer and between the continent and the Polar Front are due to sea-ice formation and northward advection of fresh meltwater, balancing the influence of surrounding saltier waters. Hence the characteristics of this mode are fundamentally due to the seasonal sea-ice melt cycle. As the ridge of surface water including AAMW is made fresh mainly by sea-ice melt, winter cooling spreads the water masses over a range of temperatures, renewing the temperature minimum layer near the Polar Front at about 1 °C, on down to freezing temperatures closer to the shelf.

At temperatures near 2 °C the AAMW and the temperature minimum layer have more or less the same characteristics. It might seem that the ridge of high volume extending from AAMW toward the freezing line matches the core of the temperature minimum layer, but this is not the case. The properties of the temperature minimum layer diverge from the ridge at lower temperatures, lying at higher salinity values approaching the freezing line. The structure of T-S curves and their relation to the temperature minimum layer and salinity minimum layers was discussed, for example, by Gordon (1975) for a section along 170 °E.

The net result of the splitting of the T-S relation by the seasonal ice cycle at the surface, the presence of saltier CDW at depth, and the accumulation near the freezing line, is to form, on the volumetric diagram (Fig. 2, lower), a ring of high volume, whose central area of low volumes lies roughly near 0 °C, 34.25 psu. The AAMW peak occurs at the upper left (warmer, and fresher) sector of the rim. In the central region of the ring, volume is minimal because it is derived from the more highly stratified layers near the base of the mixed layer. Both mechanical and thermodynamic forcing tend to reduce volume in this area of the T-S plane, as the wind-driven upwelling together with sea-ice fluxes produces a strong density gradient at the base of the mixed layer, thus expelling water mass from these layers and forming a volumetric low. Freshwater fluxes, including sea-ice melt and heat fluxes, move water near the surface in thermodynamic terms toward warmer fresher characteristics; Pellichero et al. (2018) quantified the water mass transformation in T-S classes due to precipitation and sea-ice melt and found a maximum convergence of water-mass transformation in the mixed layer at densities close to the density of AAMW.

3. Distribution and seasonality of AAMW

To investigate the spatial structure and seasonal cycle in greater detail we constructed a database consisting of ship, Argo, and seal-based CTD datasets (Appendix A; Pellichero et al. 2017). We extracted from this dataset all water types measured within the temperature/salinity range of AAMW. We then mapped the depth of each individual AAMW type recorded, its depth relative to the collocated mean mixed-layer depth, and the thickness of the AAMW layer found on each profile (Fig. 3).

AAMW is found over the entire circumpolar belt, in a band for the most part south of the Polar Front, with some extensions to the north (Fig. 3, upper). South of the Polar Front, AAMW lies in a depth range of less than about 150 m. It deepens northward reaching maximum depths (200–300 m) just north of the Polar Front. Thickness ranges from 100 to 200 m (Fig. 3, lower), making the AAMW layer a distinctively thick layer for the region, a characteristic of mode waters.

The northward deepening of the AAMW layer is associated with AAMW crossing the base of the mixed layer (Fig. 3, middle): south of the Polar Front AAMW is found within the mixed layer; north of the Polar Front AAMW is found as far as 100–200 m below the mixed layer. This structure is suggestive of AAMW being formed and ventilated south of the Polar Front and exported to the interior ocean, under the mixed layer, as it is transported northward across the Polar Front.

A similar structure is apparent seasonally in zonal averages of AAMW depth (Fig. 4, upper panels). The primary range of AAMW in the zonal average is between 50–60 °S, based on the central T-S values defining it. These characteristics form the bulk of the mixed layer (ML) at a given month. In addition, winter deepening, cooling, and salinification are apparent south of the ACC (Fig. 4, lower panels; also Fig. 3, middle panel). To the north of 50 °S in zonal average, the mode waters penetrate the ACC and become saltier and warmer at all seasons. The association of this penetration to the location of the Polar Front (Fig. 3, middle panel) is remarkable. Note that the latitudinal variations visible in the seasonal plots (Fig. 4) are partly due to averaging over longitudinal structure, but the large-scale north-south trends are clear. Summer-winter differences are particularly striking in salinity, consistent with summer sea-ice melt and winter freezing.

The spatial distribution of AAMW and its depth compared with that of the mixed layer undergoes a significant seasonal cycle (Fig. 5). AAMW is essentially found north of the sea-ice cover. In summer (Jan–Mar), the region between the sea-ice edge and the Polar Front is associated with a seasonal freshening and warming of the surface layer, due to the seasonal melt of sea-ice (Pellichero et al. 2017), which gives to the surface layer the hydrographic characteristics of AAMW. Consistent with this evolution, we observe a frequent occurrence of AAMW above the mixed-layer base in the region between the sea-ice edge and the Polar Front in summer (Fig. 5).

This region is subject to a northward Ekman transport, which carries some of this summer-formed AAMW toward the Polar Front. As winter approaches, lower temperatures lead to

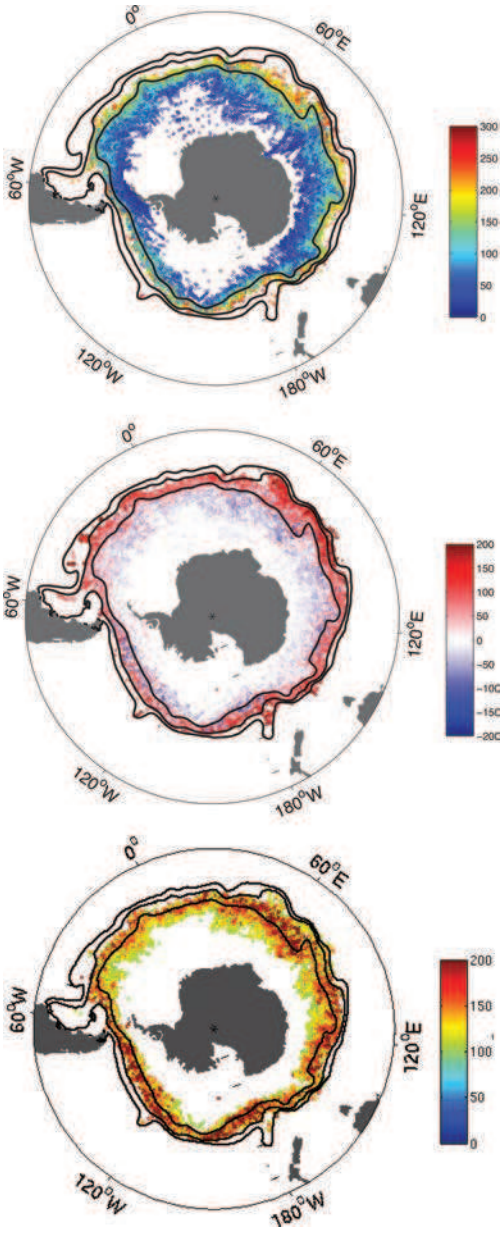

Figure 3. Depth (m) of all occurrences of AAMW found in the database (upper). Middle: depth difference (m) between AAMW depth and mixed-layer (ML) depth (calculated monthly; negative values denote AAMW above the ML base, positive denotes AAMW below the ML base). Lower: thickness (m) of AAMW layer on each individual profile of the database. The three main fronts of the ACC are indicated (black curves) from south to north: Polar Front, Subantarctic Front, northern branch of the Subantarctic Front (from Sallée et al. 2008b).

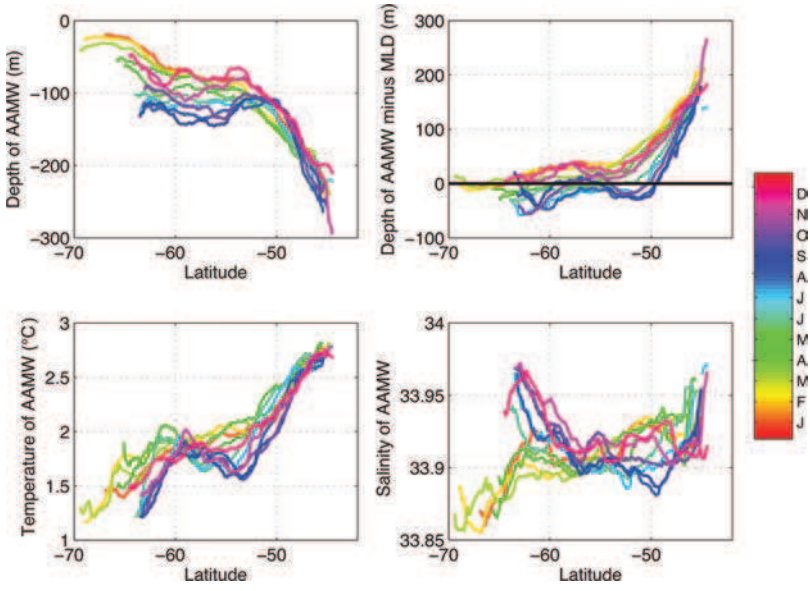

Figure 4. Monthly zonal mean characteristics of AAMW: (upper left) depth (m); (upper right) depth difference with MLD (m; negative values denote AAMW above the ML base, positive below the ML base); (bottom left) temperature (°C); (bottom right) salinity. Note that monthly time progresses upward in the color scale: winter colors are blue and summer colors are red.

sea-ice formation and an increase in salinity of the under-sea-ice surface layer, tending to remove it from the AAMW classes; hence, as the sea-ice cover extends northward, the band of mixed-layer water associated with AAMW properties becomes narrower. In winter, when sea-ice extent is at its maximum, the region where AAMW is found is restricted to the band surrounding the Polar Front (Fig. 5). The southernmost limit of this winter AAMW is still ventilated because winter mixed layers at Polar Front are relatively deep (typically ∼150–200 m; Pellichero et al. 2017), and the AAMW lies within the mixed layer for the most part (Fig. 5, upper right).

In spring (Oct–Dec), the mixed-layer depth moderates, and the AAMW layer occurs at the base of the new, shallower mixed layer south of the Polar Front. Farther north, it lies below the base of the mixed layer, with monthly occurrences concentrated in the Atlantic and Indian sectors. As summer progresses, the AAMW characteristics are frequently found beneath the mixed layer at other locations around the ACC.

The density of the AAMW, centered at about 27.1 in neutral density, together with its temperature-salinity characteristics (Fig. 1, lower panel) locates this water mass at the upper boundary of the salinity minimum layer spreading into the interior as Antarctic Intermediate Water. Also associated with AAIW, but less well recognized, is the spreading of high PV from the ML base. This spreading operates over somewhat greater density range,

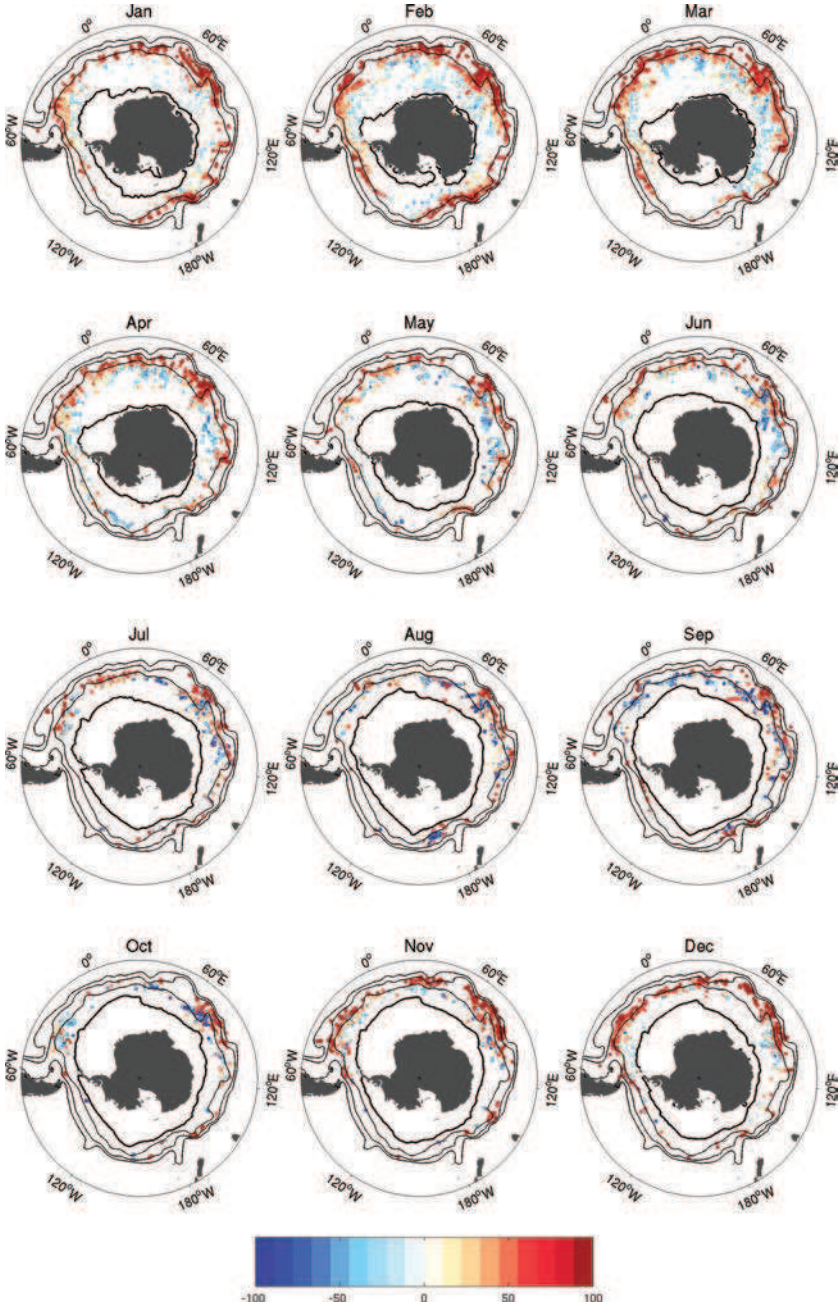

Figure 5. Depth difference (m) between AAMW depth and mixed-layer depth for each month (Jan–Dec, reading left to right, and top-down, i.e., March is at the upper right corner). Negative denotes AAMW above the ML base; Positive denotes AAMW below the ML base. Thin black curves represent the three main fronts of the ACC, from south to north: Polar Front, Subantarctic Front, and northern branch of the Subantarctic Front (Sallée et al. 2008b). Thick black curve represents the climatological sea-ice extent for a given month.

encompassing the density of the large-scale influence of AAIW across the ACC. The ML base stratification, effectively a PV barrier between the interior and surface winter mixed layer, nearly vanishes at the density of the AAMW (near 55 °S) in Figure 1 and remains weak northward across the ACC to 47 °S or so. The longitude of the section displayed in Figure 1 is about 160 °W, the region of formation of very dense varieties of Subantarctic Mode Water (Sallée et al. 2008a). In other sectors of the Southern Ocean the SAMW is less dense and well separated from AAIW.

4. Discussion

Water mass volume is determined from the Argo database in the upper 2,000 m of the Southern Ocean. Deep layer resolution is limited by the 2,000-m depth limit of the Argo data; nevertheless, water mass volume is dominated by the Upper Circumpolar Deep Water layer. Warmer branches of high volume reflect the presence of Subantarctic Mode Waters spanning a large range of temperatures. At the lowest temperatures, a prominent peak near the freezing point and 34.4 psu represents deep mixed layers in the Antarctic Slope Front and on the shelf. Maxima at higher salinity arise from the formation of dense shelf water as water accumulates in the near surface mixed layer at salinities along the freezing line up to the point that they become involved in bottom water formation.

Surface water mass formation by air-sea fluxes and the sea-ice freeze/melt cycle generates a wide variety of cold water types, and mixing with surrounding water in different regions produces distinct ridges on the volumetric diagram. A volumetric mode near 2 °C, 33.9 psu represents a kind of polar mode water. This water mass lies mainly near the Polar Front and experiences a seasonal convective cycle, apparent from the temperature minimum layer, but remains confined to relatively shallow depths compared with other mode waters owing to the net annual buoyancy gain from air-sea fluxes and ice melt. Seasonal variability of AAMW temperature and salinity is minimal in the latitude range of 50–60 °S, where its zonal mean depth shows the most variation and the least difference with the surface mixed-layer base depth. Thus, the AAMW is comprised of mixed layers south of the Polar Front and partially of waters subducted below the Polar Front.

Upwelling over the Antarctic Zone thins the surface layer, and the buoyancy gain in this region roughly balances northward Ekman transport of cold water. Hence, as already noted, the surface forcing does not lead to a deep convective layer. The depth of the surface mixed layer nevertheless increases on average approaching the Polar Front, and into the AAMW. What, then, sets the scale for the depth of the AAMW? The Ekman transport itself causes some vertical mixing and deepening north of the Polar Front (Rintoul and England 2002). South of the Polar Front, however, this effect is muted by weak horizontal density gradients at the surface. Instead, the vertical motion of isopycnal surfaces below the mixed layer driven by the Ekman suction may be balanced by lateral eddy fluxes.

To examine this idea, we use a relation that is essentially a residual circulation model like that used by Marshall and Radko (2003; see also Marshall 1997; Olbers and Visbeck 2005) in their analysis of the role of eddy effects on the structure of the ACC. Focusing on a single isopycnal surface, with variations in the meridional direction, the equation for the change in depth of this isopycnal due to upwelling and eddy mass flux may be written as follows:

$$\frac{\partial z_\rho}{\partial t} = W + K\frac{\partial^2 z_\rho}{\partial y^2}$$

with z_ρ as the depth to an isopycnal that lies at a mean depth of z_0 some distance below the Ekman layer and by assumption not impacted by convection, and where W is the vertical velocity at the depth of the isopycnal surface and K is the eddy diffusion coefficient.

Setting the scale for the vertical velocity as the Ekman velocity, the scale for the depth perturbation is $\delta h \sim L^2 \frac{W_{Ek}}{K}$, which is 200 m for $L \sim 1{,}000$ km, $w_0 \sim 10^{-6}$ m/s, and $K \sim 5 \times 10^3 \mathrm{m}^2/\mathrm{s}$. The Ekman pumping W_{Ek} scales directly with the wind stress; hence, this relation represents a depth scale that increases proportionally in response to wind and decreases in response to eddy diffusion, supposed here to be relatively large near the surface.

Recognizing that the strength of the eddy diffusion may itself vary with wind, for example, through a dependence of eddy kinetic energy on wind (see, e.g., Meredith et al. 2012), the relation between wind and the depth scale changes. Assuming an eddy diffusion coefficient that varies with wind as $K \sim \tau^{1/2}$, where τ is the wind stress, leads to a weaker perturbation depth scale dependence on wind as $\delta h \sim \tau^{1/2}$. A weaker dependence on wind implies less sensitivity to variations in wind stress, and a more uniform circumpolar distribution of mode water, similar to that observed. AAMW depth is not exactly uniform, of course, with values roughly 100 m greater in the Indian Ocean sector where mean winds are stronger than those in the eastern Pacific sector (Fig. 3).

More generally, AAMW properties are set by the large-scale balance of northward advection of water and ice with lateral mixing. This water mass forms the upper boundary of the AAIW layer and controls the circumpolar distribution of that water mass along the Polar Front. The role of cross-frontal exchange and, in somewhat different terms, the incursion of the temperature minimum layer into the Subantarctic zone has been noted before: Gordon et al. (1977) discussed the likely role of these effects on the thermohaline structure of the Scotia Sea. The volumetric estimate leading to the identification of AAMW provides a straightforward measure of the impact of cross-frontal circulation and lateral thermohaline fluxes near the Polar Front, and is directly linked to the large-scale stratification of the intermediate layers of the ACC.

Acknowledgments. K.S. would like to acknowledge support from NSF OCE 1231803, NSF OCE 0622670, and NSF OCE 0822075. JBS has received funding from the European Research Council (ERC) under the European Union's Horizon 2020 research and innovation program (grant agreement 637770).

Appendix A

We briefly describe the data inventory based on individual profiles in the database. A full description and discussion of the seasonal mixed layer evolution, heat, and freshwater balances is given in Pellichero et al. (2017). To illustrate the data coverage for the volumetric calculation we display an inventory of the number of profiles of different sources in summer (November to April) and winter (May to October) seasons (ship, Argo, seals; Fig. A1). Figure A1 highlights the complementarity of the three sources of observations

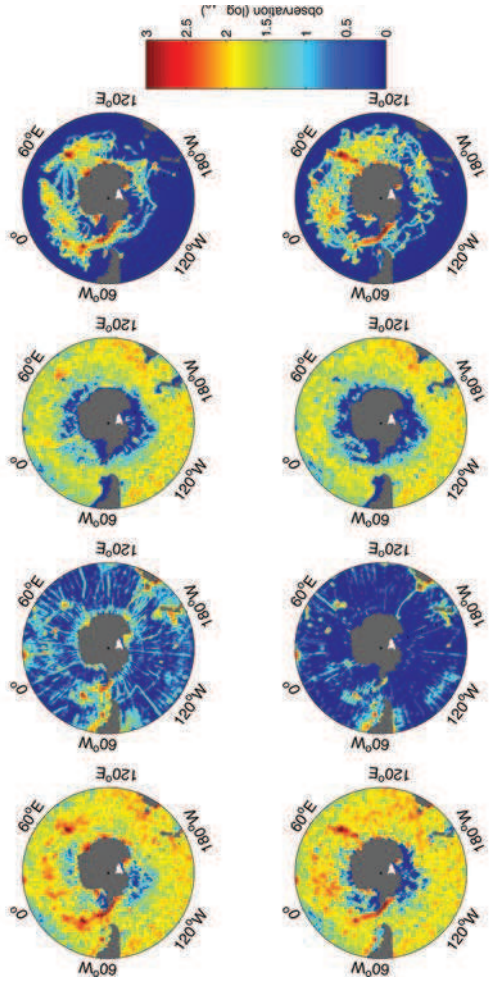

Figure A1. Number ($\log_{10}$) of individual profiles in 2 × 2 bins (longitude, latitude) in the database in summer (upper; November to April), and in winter (lower; May to October). Number of profiles in the entire combined database is shown (first column from the left), as well as for ship-based (second column), Argo profiles (third column), and elephant seal (forth column).

and the relatively good coverage both in summer and winter. Figure A2 details the monthly observation coverage. Argo float data provide large-scale coverage throughout the year away from dense sea-ice concentrations, whereas seal-based data complement Argo sampling in the sea-ice zone in both summer and winter and provide relatively dense sampling across the full extent of the seasonal sea-ice in a few regions.

Figs. A2, A3, and Figs. 3–5 show frontal locations based on the definition in Sallée et al. 2008b. These definitions produce a result similar to the traditional definition of the Polar Front (PF) as the northern limit of the Antarctic Winter Water (AAWW) defined as the tongue of 2 °C water at 200 m (Orsi et al. 1995; Belkin and Gordon 1996). Clearly, the hydrographic definition of the Polar Front is closely related to the properties of the AAMW identified based on temperature-salinity characteristics.

The Subantarctic Front can be defined as the maximum in the meridional gradient of temperature, density, or potential vorticity (PV). Belkin and Gordon (1996) define the SAF as the maximum temperature gradient at 300 m (T300m). These rules separate the Antarctic zone from the subantarctic zone by definition, with strong gradients separating the colder, fresher Antarctic zone from the warmer saltier subantarctic region.

To complete the description of the database for the mode water distribution we also display monthly mixed-layer depth where the mixed layer shows the characteristics of AAMW (Fig. A3). Late winter mixed-layer depths are greatest upstream of the Kerguelen Plateau, where a strong divergence of multiple polar frontal zones is generated by several seamounts (Sallée et al. 2008b). This is also the region of stronger mean wind stress.

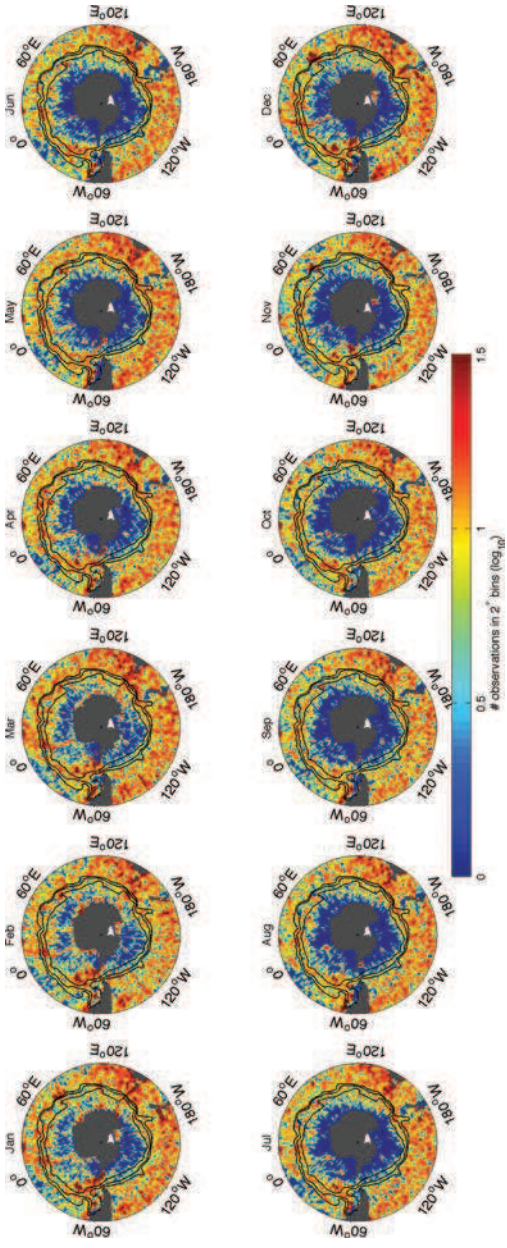

Figure A2. Number ($\log_{10}$) of individual profiles in 2×2 bins (longitude, latitude) in the combined database for each month of the year. Black curves represent the three main fronts of the ACC, from south to north: Polar Front, Subantarctic Front, northern branch of the Subantarctic Front (Sallée et al. 2008b).

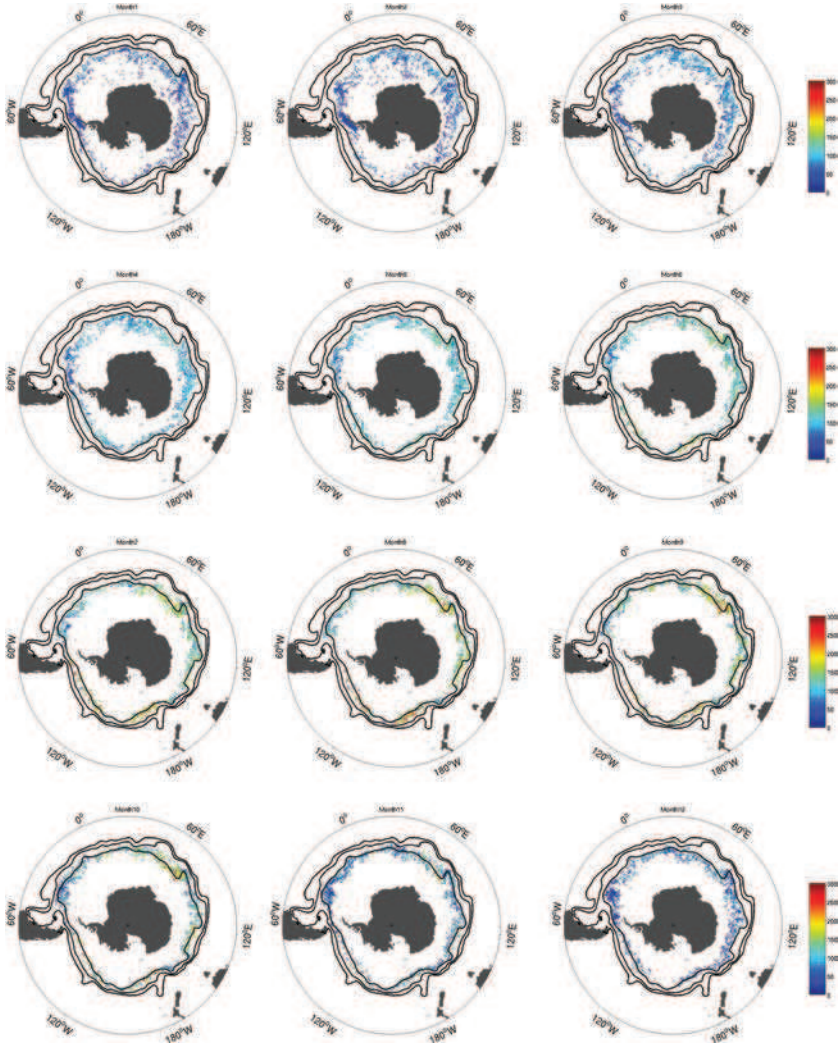

Figure A3. Monthly mixed-layer depth for all occurrences of an ML found with the characteristics of AAMW. January is at the upper left (Month1) proceeding through to December (Month12) at the lower right. Black curves represent the three main fronts of the ACC, from south to north: Polar Front, Subantarctic Front, northern branch of the Subantarctic Front (Sallée et al. 2008b).

REFERENCES

Aoki, S., S. R. Rintoul, H. Hasumoto, and Hideki Kinoshita. 2006. Frontal positions and mixed layer evolution in the Seasonal Ice Zone along 140°E in 2001/02. Polar Biosci., 20, 1–20.

Behrendt, A., E. Fahrbach, M. Hoppema, G. Rohardt, O. Boebel, O. Klatt, A. Wisotzki, and H. Witte. 2011. Variations of Winter Water properties and sea ice along the Greenwich meridian on decadal time scales, Deep Sea Res. Part 2 Top. Stud. Oceanogr., 58, 25–26: 2524-2532. doi: 10.1016/j.dsr2.2011.07.001

Belkin, I. M. and A. L. Gordon. 1996. Southern Ocean fronts from the Greenwich Meridian to Tasmania. J. Geophys. Res., 101, 3675–3696.

Boyer, T.P., J. I. Antonov, O. K. Baranova, C. Coleman, H. E. Garcia, A. Grodsky, D. R. Johnson, et al. 2013. World Ocean Database 2013. NOAA Atlas NESDIS 72. Silver Spring, MD: NOAA. 209 pp. doi: 10.7289/V5NZ85MT

Carmack, E. C. 1977. Water characteristics of the Southern Ocean south of the Polar Front, *in* A Voyage of Discovery, M. Angel ed. G. Deacon 70th Anniversary Volume, Supplement to Deep-Sea Res. New York: Pergamon Press. pp. 15–42.

Cerovečki, I., L. D. Talley, M. R. Mazloff, and G. Maze. 2013. Subantarctic mode water formation, destruction, and export in the eddy-permitting Southern Ocean State Estimate. J. Phys. Ocean., 43, 1485–1511. doi: 10.1175/JPO-D-12-0121.1

Dong, S., J. Sprintall, S. T. Gille, and L. Talley. 2008. Southern Ocean mixed-layer depth from Argo float profiles. J. Geophys. Res., 113, C06013. doi: 10.1029/2006JC004051

Dong, S., S. L. Garzoli, and M. Baringer. 2009. An assessment of the seasonal mixed layer salinity budget in the Southern Ocean, J. Geophys. Res., 114. doi: 10.1029/2008JC005258

Dong, S., J. Sprintall, and S. Gille. 2007. An assessment of the Southern Ocean mixed layer heat budget. J. Clim. 20, 4425–4442. doi: 10.1175/JCLI4259.1

Fahrbach, E., G. Rohardt, M. Schröder, and V. Strass. 1994. Transport and structure of the Weddell Gyre. Ann. Geophys., 12, 840–855.

Faure, V., M. Arhan, S. Speich, and S. Gladyshev. 2011. Heat budget of the surface mixed layer south of Africa. Ocean Dyn., 61, 1441–1458. doi: 10.1007/s10236-011-0444-1

Gordon, A. L. 1971. Oceanography of Antarctic Waters, Antarctic Oceanology I. Antarct. Res. Ser., vol. 15, J. L. Reid ed. Washington, DC: AGU. pp. 169–203.

Gordon, A. 1975. An Antarctic oceanographic section along 170°E. Deep-Sea Res., 22, 357–377. doi: 10.1016/0011-7471(75)90060-1

Gordon, A. L., D. T. Georgi, and H. W. Taylor. 1977. Antarctic Polar Frontal Zone in the Western Scotia Sea – Summer 1975. J. Phys. Oceanogr., 7, 309–328.

Gordon, A. L., C. T. A. Chen, and W. G. Metcalf. 1984. Winter layer entrainment of Weddell Deep Water. J. Geophys. Res., 89, 637–640.

Gordon, A. L. and B. A. Huber. 1984. Thermohaline stratification below the Southern Ocean sea ice. J. Geophys. Res., 89, 641–648.

Gordon, A. L. and B. A. Huber. 1990. Southern Ocean winter mixed layer. J. Geophys. Res., 95, 11655–11672.

Hanawa, K., and L. Talley. 2001. Mode waters, *in* Ocean Circulation and Climate. International Geophysics Series, G. Siedler and J. Church, eds. London: Academic Press. pp. 373–386.

Marshall, D. 1997. Subduction of water masses in an eddying ocean. J. Mar. Res., 55, 201–222.

Marshall, J. and T. Radko. 2003. Residual-mean solutions for the Antarctic Circumpolar Current and its associated overturning circulation. J. Phys. Oceanogr., 33, 2341–2354.

Meredith, M. P., A. C. Naveira Garabato, A. M. Hogg, and R. Farneti. 2012. Sensitivity of the overturning circulation in the Southern Ocean to decadal changes in wind forcing. J. Clim., 25, 99–110. doi: 10.1175/2011JCLI4204.1

Olbers, D. and M. Visbeck. 2005. A model of the zonally averaged stratification and overturning in the Southern Ocean. J. Phys. Oceanogr., 35, 1190–1205. doi: 10.1175/JPO2750.1

Orsi, A. H., T. Whitworth, III, and W. D. Nowlin, Jr. 1995. On the meridional extent and fronts of the Antarctic Circumpolar Current. Deep Sea Res. Part I, 42, 641–673.

Park, Y.-H., E. Charriaud, and M. Fieux. 1998. Thermohaline structure of the Antarctic surface water/winter water in the Indian sector of the Southern Ocean. J. Mar. Syst., 17(1–4), 5–23. doi: 10.1016/S0924-7963(98)00026-8

Pellichero, V., J.-B. Sallée, S. Schmidtko, F. Roquet, and J.-B. Charrassin. 2017. The ocean mixed layer under Southern Ocean sea-ice: seasonal cycle and forcing, J. Geophys. Res. Oceans, 122, 1608–1633. doi: 10.1002/2016JC011970

Pellichero, V., J. B. Sallée, C. Chapman, and S. Downes. 2018. The Southern Ocean meridional overturning in the sea-ice sector is driven by freshwater fluxes. Nat. Commun., 9, 1789.

Petty, A. A., P. R. Holland, and D. L. Feltham. 2014. Sea ice and the ocean mixed layer over the Antarctic shelf seas. Cryosphere, 8, 761–783. doi: 10.5194/tc-8-761-2014

Ren, L., K. Speer, and E. P. Chassignet. 2011. The mixed layer salinity budget and sea ice in the Southern Ocean. J. Geophys. Res., 116, C08031. doi: 10.1029/2010JC006634

Rintoul, S. and M. England. 2002. Ekman transport dominates air–sea fluxes in driving variability of Subantarctic Mode Water. J. Phys. Oceanogr., 32, 1308–1321.

Sallée, J.-B., N. Wienders, K. Speer, and R. Morrow. 2006. Formation of Subantarctic mode water in the southeastern Indian Ocean. Ocean Dyn., 56, 525–542. doi: 10.1007/s10236-005-0054-x

Sallée, J.-B., R. Morrow, and K. Speer. 2008a. Eddy heat diffusion and Subantarctic Mode Water formation. Geophys. Res. Lett. 35, L05607. doi: 10.1029/2007GL032827

Sallée, J.-B., K. Speer, and R. Morrow. 2008b. Response of the Antarctic Circumpolar Current to atmospheric variability. J. Clim., 12, 3020–3039. doi: 10.1175/2007JCLI1702.1

Sallée, J.-B., K. Speer, S. Rintoul, and S. Wijffels. 2010a. Southern Ocean thermocline ventilation. J. Phys. Oceanogr. 40, 509–529. doi: 10.1175/2009JPO4291.1

Sallée, J.-B., K. Speer, and S. R. Rintoul. 2010b. Zonnally asymmetric response of the Southern Ocean mixed-layer depth to the Southern Annular Mode. Nat. Geosci., 3, 273–279. doi: 10.1038/ngeo812

Schmidtko, S., G. C. Johnson, and J. M. Lyman. 2013. MIMOC: a global monthly isopycnal upper-ocean climatology with mixed layers. J. Geophys. Res.: Oceans, 4. doi: 10.1002/jgrc.20122

Speer, K. and G. Forget. 2013. Global distribution and formation of mode waters, *in* Ocean Circulation and Climate, A 21st Century Perspective, 2nd ed., G. Siedler, S. Griffies, J. Gould, and J. Church, eds. International Geophysics Series, Volume 103. Cambridge, MA: Academic Press.

Toole, J. 1981. Sea ice, winter convection, and the temperature minimum layer in the Southern Ocean. J. Geophys. Res., 86, 8037–8047.

Whitworth, T., III, A. H. Orsi, S.-J. Kim, W. D. Nowlin, Jr., and R. A. Locarnini. 1998. Water masses and mixing near the Antarctic Slope Front, *in* Ocean, Ice, and Atmosphere: Interactions at the Antarctic Continental Margin, S. S. Jacobs and R. F. Weiss, eds. Antarctic Research Series, Volume 75. Washington, DC: American Geophysical Union. pp. 1–27.

Worthington, L. V. 1981. The water masses of the world ocean: some results of a fine-scale census, *in* Evolution of Physical Oceanography, Scientific Surveys in Honor of Henry Stommel, B. A. Warren and C. Wunsch, eds. Cambridge, MA: MIT Press. pp. 42–69.

Received: *28 February 2018*; revised: *24 October 2018*.